Chapter 3. Results

3.1. *rho-1* regulates epidermal elongation in *C. elegans* embryogenesis

3.1.1 Zygotic *rho-1* is required for elongation

Elongation is driven by actin-myosin contraction in the seam cells, which changes their shape from cuboidal to cylindrical and causes a 4-fold increase in the length of the embryo (Chisholm and Hardin, 2005). These contractions are controlled by Rho kinase/LET-502, which is highly expressed in the seam cells and is required for nonmuscle light chain phosphorylation (Wissmann et al., 1997; Piekny et al., 2000; Piekny and Mains, 2002). In higher eukaryotes, Rho kinase is a downstream effector of active RhoA, and we hypothesize that *C. elegans* RhoA/RHO-1 also has a role in elongation. In support of this, embryos mutant for *rga-2*, which encodes a GAP (GTPase activating protein) for RHO-1, show elongation phenotypes similar to *mel-11* (myosin phosphatase regulatory subunit) mutants, where embryos rupture likely due to hypercontractility (Diogon et al., 2007). A function for *rho-1* in elongation had not been determined due to its maternal requirement for cytokinesis and the lack of zygotic alleles. Recently, a deletion allele of *rho-1*, *ok2418,* was generated by the Knockout Consortium, and consists of a 2091bp deletion that removes aas 53-192. The remaining portion of the protein (1-52 amino acids) is considered null, as it would not be able to function biochemically (Dvorsky and Ahmadian, 2004). This allele was used to determine if *rho-1* is required for elongation and to ascertain *rho-1*'s placement in the pathway.

First, we assessed the phenotype of *rho-1 (ok2418)* homozygous embryos. Embryos from hermaphrodites heterozygous for *rho-1* (over a wild type chromosome or mutant for *dpy-4*) segregated 76% wt or Dpy worms and the homozygous *rho-1* mutant

embryos were lethal (15.1%) or arrested as Lpy Dpy larvae (8.9%; Table 1). Live imaging was performed with embryos from *rho-1/dpy-4* heterozygous hermaphrodites to obtain a better assessment of their phenotypes. Approximately 20% of the progeny (*rho-1* homozygous embryos, n≥300) arrested at the 1.5-2-fold stage of elongation during embryogenesis (Figure 11). Some of these embryos hatched the next day and arrested as Lpy Dpy larvae. A 1.5-2-fold arrest is commonly observed with mutations in genes that regulate embryonic elongation, but can also arise from mutations in genes that form muscle or muscle attachments (e.g. pats – paralyzed at two-fold; Zhang and Labouesse, 2010; Zhang et al., 2010).

To better assess the *rho-1* phenotype, mutant embryos were filmed using a marker for the adherens junctions of epidermal cells. A strain heterozygous for the *rho-1 (ok2418)* allele and expressing AJM-1::GFP (adherens junction marker) was generated and embryos from these worms were imaged using fluorescence microscopy (performed by Y. Chen). AJM-1 is found at cell-cell junctions and serves as a good tool to observe cell shape changes as it outlines the epidermal cells. AJM-1 localization in homozygous *rho-1 (ok2418)* embryos resembled wild-type embryos during early stages of elongation (comma-1.5-fold stage), but the *rho-1* homozygous embryos did not elongate past the 2-fold stage and the shape of the seam cells did not fully change into long cylindrical shapes (by Y. Chen; Figure 12). This result suggests that the epidermal cells are born and adhere properly in *rho-1* mutant embryos, but the lateral epidermal cells are not able to extend beyond a certain length.

3.1.2. RHO-1 localizes to the boundaries of epidermal cells

Table 1. *rho-1* may function in the pathway that controls embryonic elongation.

Parental Genotype	℃ Temp	% Hatching	% Embryonic lethality*	% Elongation Phenotype^
N2 (wt)	20	100	0	0
rho-1(ok2418)/dpy-4(e1166)	20	84.9	15.1	8.9
mlc-4(or253)/qC1	20	94.4	5.6	24.2
mlc-4(or253)/+;rho-1(ok2418)/+	20	82.7	17.3	20.8
let-502(sb118ts)	20	95.2	4.8	0
let-502(sb118ts)/+;rho-1(ok2418)/+	20	82.2	17.8	7.8
let-502(sb118ts);rho-1(ok2418)/+	20	Sterile: low brood size		
mel-11(it26ts)	15	20	80	0
mel-11(it26ts)	20	8.8	91.2	0
mel-11(it26ts)	25	0	100	0
mel-11(it26ts); rho-1(ok2418)/+ or rho-1(ok2418)	15	31	69	2
mel-11(it26ts); rho-1(ok2418)/+ or rho-1(ok2418)	20	15.6	84.4	0
mel-11(it26ts); rho-1(ok2418)/+ or rho-1(ok2418)	25	Sterile: low brood size		
rhgf-2(sb100)	20	99.9	0.01	0
rhgf-2(sb100)/+; rho-1(ok2481)/+	20	75.7	24.3	6.7
rhgf-2(sb100); rho-1(ok2481)	20	73	27	11

n > 300 embryos and larva per cross except for *rhgf-2(sb100); rho-1(ok2481)*, n = 167 (performed with Y. Chen).

* Embryonic lethality includes embryos arrested at different stages.

^ Elongation phenotypes include Lpy Dpy

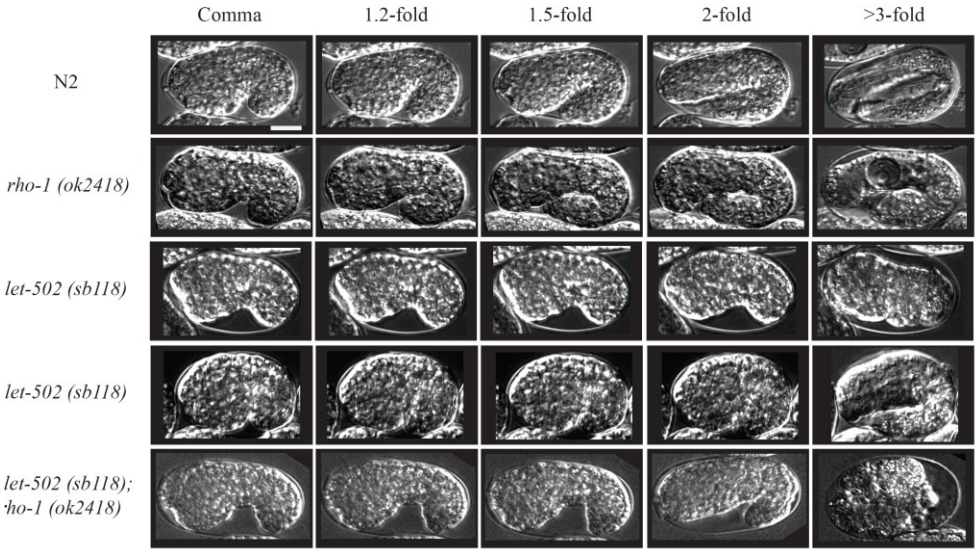

Figure 11. *rho-1* is required for elongation. DIC images from time lapse movies of N2, *rho-1 (ok2418)*, *let-502 (sb118)* and *let-502(sb118); rho-1 (ok2418)* embryos from comma stage (just after ventral enclosure has completed) to past the 3-fold stage of elongation. All imaging was done at room temperature (22°C). Scale bar is 10 μm.

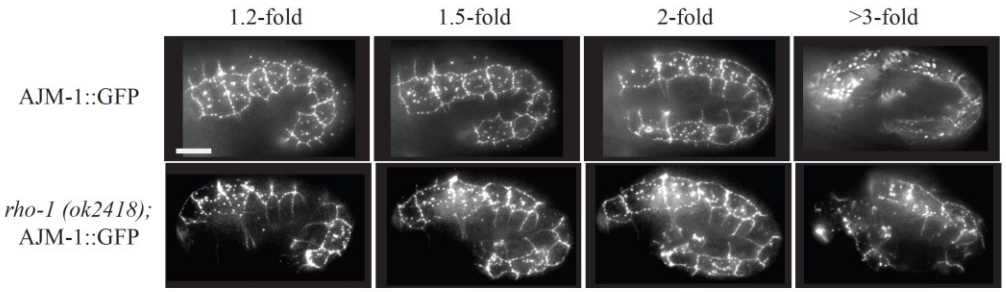

Figure 12. *rho-1* is required for epidermal cell shape changes during elongation. Fluorescent images from time lapse movies of AJM-1::GFP and *rho-1 (ok2418);*AJM-1::GFP embryos from early elongation (1.2-fold stage) to just past the 3-fold stage of elongation are shown. Scale bar is 10 μm. Movies performed by Y. Chen.

If *rho-1* is genetically required for elongation, then it should be enriched in the lateral epidermal cells. Unfortunately there are no anti-RHO-1 antibodies that work for immunofluroescence, nor is there a GFP::RHO-1 transgenic strain containing the *rho-1* promoter. However, there is a GFP::RHO-1 strain that is controlled by the maternal promoter for *pie-1*. The *pie-1* gene is maternally expressed and is required for establishing cell fates in the early embryo (Curran et al. 2009). Although it is not well understood why, the *pie-1* promoter permits germline expression, while many other promoters are repressed. Therefore, using the *pie-1* promoter enables the visualization of proteins of interest. GFP::RHO-1 localized to the boundaries of all epidermal cells during dorsal intercalation, ventral enclosure, and elongation (Figure 13). This result suggests that maternal RHO-1 is very stable and persists through the early stages of elongation.

3.1.3. *rho-1* is part of the elongation pathway

The phenotype of *rho-1* homozygous embryos supports its requirement for elongation, likely as a regulator of myosin contractility. To place *rho-1* in this pathway, crosses were performed with strains carrying mutations in genes of the elongation pathway, and hatching rates and/or % of larval Lpy Dpy phenotypes were determined. The interaction between two genes was considered to be enhanced if the observed lethality for the double mutant exceeded predicted additive lethality rates for each mutant on its own, as determined by the Chi-square analysis ($p > 0.05$). More specifically, the *rho-1* allele, *ok2418,* was crossed with mutations in *mlc-4* (nonmuscle myosin regulatory light chain), *let-502* (Rho kinase), *mel-11* (myosin phosphatase regulatory subunit) and *rhgf-2* (GEF). Hermaphrodites heterozygous for both *mlc-4 (or253*; a zygotic null allele)

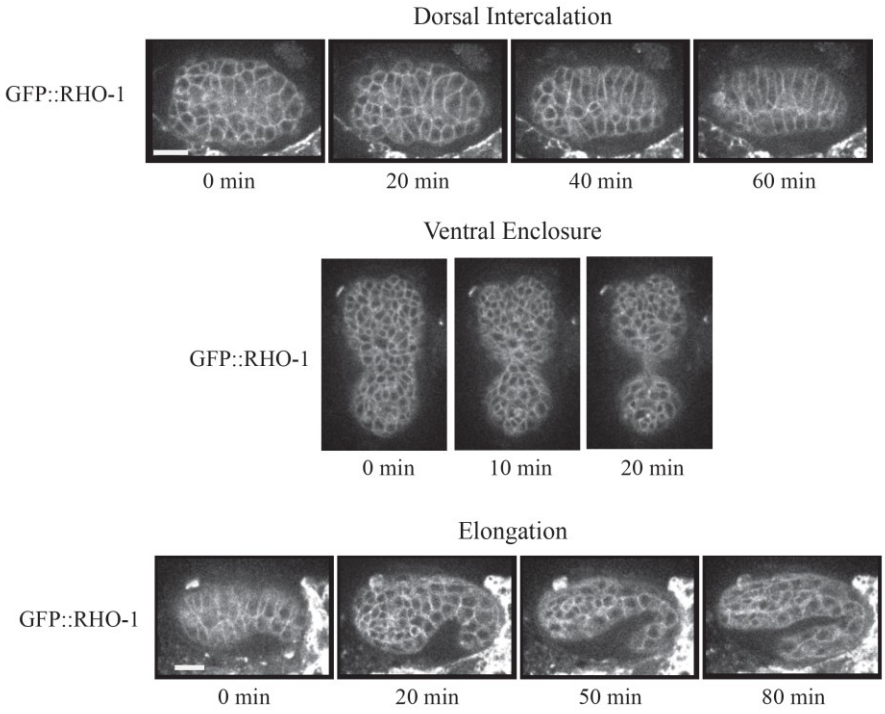

Figure 13. *rho-1* localizes to epidermal cell boundaries. Fluorescent images from time lapse movies of GFP::RHO-1 embryos show GFP::RHO-1 localization at the boundaries of epidermal cells during dorsal intercalation, ventral enclosure and elongation as indicated. Scale bar is 10 μm.

and *rho-1 (ok2418)* segregated progeny with phenotypes that matched the predicted frequencies for each allele (Table 1). The lack of enhancement between the null alleles supports that *mlc-4* (nonmuscle myosin regulatory light chain) and *rho-1* (Rho kinase) function in the same pathway.

Crosses were also performed to determine if *rho-1* and *let-502* genetically interact. The *let-502* allele, *sb118*, is a hypomorphic temperature sensitive (ts) allele with high viability at 20°C (95%). Hermaphrodites heterozygous for both alleles segregated progeny with phenotypes that matched the predicted frequencies for each allele, suggesting that *rho-1* and *let-502* function in the same pathway (Table 1). Live imaging of *let-502 (sb118); rho-1 (ok2418)* embryos revealed elongation phenotypes similar to severe *let-502 (sb118)* embryos (Figure 11). Also, *let-502 (sb118); rho-1 (ok2418)/+* hermaphrodites had low brood sizes (Table 1; performed together with Y. Chen). This enhancement could suggest that *rho-1* has some haploinsufficiency, which is only revealed when it is in combination with a partial loss of maternal *let-502.*

To further assess *rho-1*'s placement in the elongation pathway, the *rho-1* mutant was crossed with a mutation in *mel-11* (myosin phosphatase regulatory subunit). *mel-11 (it26)* is a ts allele that shows embryonic lethal phenotypes at 15 ^{o}C (20% hatching) and 20 ^{o}C (2% hatching), due to rupturing of the embryo during elongation likely because of increased contractility in the epidermal cells. Embryonic lethality of *mel-11 (it26)* was partially suppressed by *rho-1 (ok2418)* (or *rho-1 (ok2418)/+*) at 15 ^{o}C (31% hatching) and 20 ^{o}C (16% hatching; Table 1; performed together with Y. Chen). In addition, a small number of embryos displayed larval Lpy Dpy phenotypes and 2-fold arrest, similar to the *rho-1* phenotype. Although the *mel-11* allele is not null, this result suggests that *rho-1*

and *mel-11* function antagonistically and *rho-1* is epistatic to *mel-11*. As an upstream regulator of Rho kinase and myosin contractility, reducing *rho-1* function could alleviate the hypercontractility caused by the removal of myosin phosphatase.

Lastly, *rho-1* was tested for genetic interactions with a hypomorphic allele of *rhgf-2*, which encodes a GEF for RHO-1 (Lin et al. 2012). The hatching rates were slightly lower for the double mutants in comparison to each mutant on its own, supporting weak enhancement between *rho-1* and *rhgf-2* (Table 1; performed with Y. Chen). It is not clear why there is some enhancement between *rho-1* and *rhgf-2*, which could occur if RHGF-2 also functions in a parallel pathway. However, the potential overlapping requirement for both maternal and zygotic *rho-1* during elongation could also explain the enhancement. Live imaging revealed that the elongation defects of the *rhgf-2 (sb100); rho-1 (ok2481)* embryos (data not shown) were similar to *rho-1 (ok2418)* embryos, as expected if *rhgf-2* is an upstream activator of *rho-1*.

Together, these data support a role for *rho-1* in elongation. The two-fold arrest phenotype that arises from the zygotic null allele, coupled with its genetic interactions with various components of the elongation pathway indicates that RHO-1 is an upstream regulator of myosin contractility.

3.2. *ani-1* is non-autonomously required for ventral enclosure during *C. elegans* embryogenesis

3.2.1 *ani-1* is required throughout embryogenesis

ANI-1 shares homology with human anillin, which has binding sites for both F-actin and active myosin, and is hypothesized to organize actin-myosin contractility in the

early embryo (Maddox et al., 2007; Tse et al., 2011). Elongation also requires actin-myosin contractility within the lateral epidermal cells to drive their shape change. In addition, other events in epidermal morphogenesis, including dorsal intercalation and ventral enclosure may also require actin-myosin contractility for cell migration and shape changes.

To determine if *ani-1* is required for epidermal morphogenetic events during embryogenesis, N2 hermaphrodites were treated with *ani-1* RNAi. Depletion of *ani-1* gave 43% embryonic lethality and 13.4% larval Lpy Dpy phenotypes (Table 2). The Lpy Dpy phenotype signifies abnormal body morphology and presumably arises due to defects in epidermal morphogenesis. To better assess the embryonic phenotypes, *ani-1* RNAi embryos were imaged throughout development. A large percentage (51.6%, normalized from lethal embryos) of embryos displayed early phenotypes (amorphous ball of cells with no obvious structures), likely due to failed polar body extrusion or cytokinesis defects (Maddox et al., 2007; Dorn et al., 2010). However, the remaining embryos displayed defects later in development, including ventral enclosure and elongation (Figure 14). The range from early to late phenotypes supports that *ani-1* is required throughout embryogenesis, and this data supports that it may regulate epidermal morphogenesis.

Since *ani-1* is required maternally for polar body extrusion (Dorn et al., 2010) and cytokinesis (Maddox et al., 2005; Maddox et al., 2007), we wanted to bypass these early requirements and study the zygotic-specific function of *ani-1*. To test for this, *rde-1* (RNAi-resistant) hermaphrodites were treated with *ani-1* RNAi and outcrossed to N2 males. This permitted maternal *ani-1* to be expressed due to RNAi resistance in the

Table 2. *ani-1* is required during embryogenesis.

Genotype	RNAi	% Hatching	% Embryonic Lethality	% Larval Phenotypes
N2	L4440	97.5	2.5	0
N2	*ani-1*	57	43	13.4
rde-1(ne219) X wt	L4440	100	0	0
rde-1(ne219) X wt	*ani-1*	98.7	1.3	17.6

Data was averaged from four experiments, with 4-9 hermaphrodites per experiment, and n > 300 for *ani-1* RNAi and n > 100 embryos and larva for *rde-1* treatments and crosses. Larval phenotypes include hatched Lpy Dpy embryos.

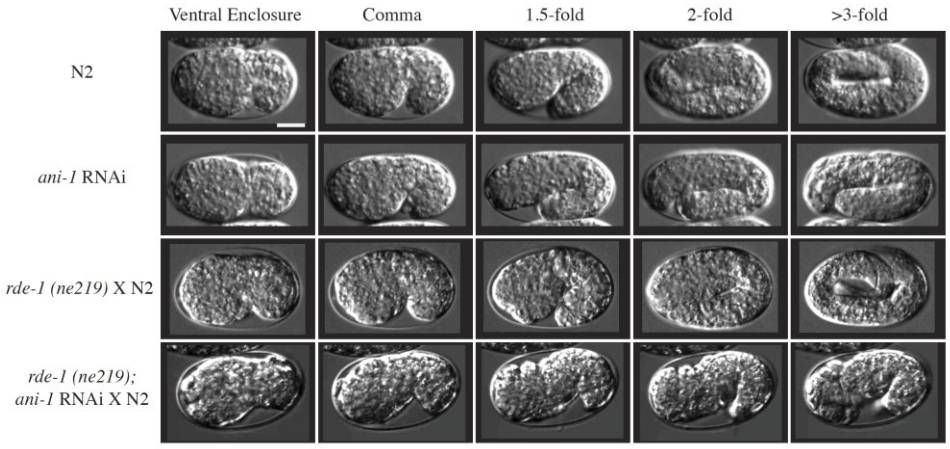

Figure 14. *ani-1* is required throughout embryogenesis. DIC images from time lapse movies of N2 and *ani-1* RNAi embryos are shown in the top two sets of panels as indicated. The movies start from ventral enclosure and continue past the 3-fold stage of elongation. *rde-1 (ne219)* hermaphrodites were treated with L4440 (vector alone control) or *ani-1* RNAi and outcrossed to N2 males. DIC images from time lapse movies of embryos are shown in the bottom two sets of panels as indicated. Scale bar is 10 μm.

mother, but zygotically expressed *ani-1* was susceptible to knockdown by RNAi. A range of 4 to 9 Lpy Dpy larva were observed on each of the mated plates, giving a total of 17.6% Lpy Dpy larva (the average brood size per plate was ~35 embryos and only first broods were considered as the RNAi was titrated out in younger oocytes; Table 2). This percentage of Lpy Dpy larva is consistent with what was observed for *ani-1* RNAi, and may reflect zygotic-specific requirements for *ani-1* in epidermal morphogenesis. In support of this, embryos imaged by DIC displayed ventral enclosure and elongation phenotypes consistent with what was observed with *ani-1* RNAi (Figure 14). These results indicate that *ani-1* is required throughout embryogenesis, and is both maternally and zygotically required for epidermal morphogenesis.

3.2.2. *ani-1* is required for ventral enclosure

Initial phenotyping of *ani-1* RNAi embryos revealed defects in epidermal morphogenesis. To better characterize *ani-1*'s role in this process, live imaging was performed using embryos from AJM-1::GFP hermaphrodites treated with *ani-1* RNAi. As described earlier, AJM-1 marks epidermal cell boundaries, permitting the visualization of all stages of epidermal morphogenesis. Of the *ani-1* RNAi embryos that did not arrest early, 33% displayed ventral enclosure defects where the ventral cells failed to properly migrate and adhere at the ventral midline (vs. 3% of AJM-1::GFP on L4440, n = 79; Table 3 and Figure 15). For this data set, embryos were considered to have an 'early' ventral enclosure phenotype if the leading edge cells and/or posterior pocket cells failed to meet at the ventral midline (ventral epidermal cells always migrated to some degree and were not truly 'early', which is when epidermal cells fail to migrate altogether

Table 3. *ani-1* is required during ventral enclosure.

Genotype	% VE phenotypes	% WT
AJM-1::GFP; L4440	3	97
AJM-1::GFP; *ani-1* RNAi	33	67

n > 79

% phenotypes were normalized (e.g. early phenotypes not counted) to reflect the proportion of ventral enclosure (VE) phenotypes.

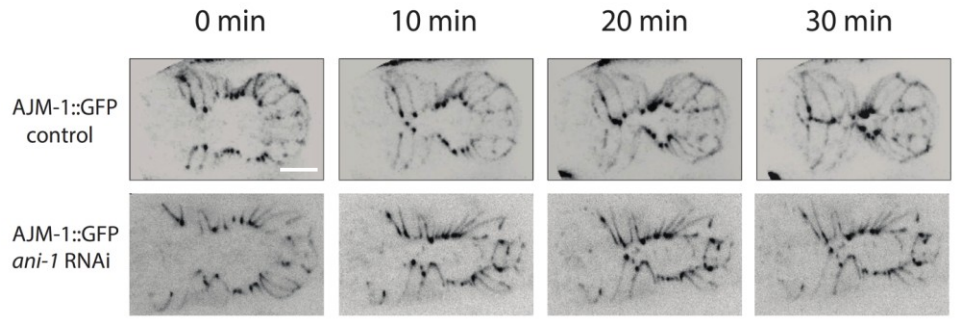

Figure 15. *ani-1* is required for ventral enclosure. Inverted fluorescent images from time lapse movies of control and AJM-1::GFP; *ani-1* RNAi embryos showing the migration of ventral epidermal cells during ventral enclosure. Z-stack projections of planes from the ventral surface are shown. Scale bar is 10 μm.

and remain on the dorsal surface; Figure 15). A 'late' ventral enclosure phenotype was when the ventral epidermal cells met at the ventral midline (resembling wild-type embryos), but failed to properly seal causing internal contents to extrude later in development (data not shown). There was an equal ratio of embryos among the early and late ventral enclosure phenotypes, suggesting that *ani-1* is required for the proper migration and/or adhesion of ventral epidermal cells (Table 4). This data also suggests that the larva Lpy Dpy phenotypes may reflect weak ventral enclosure phenotypes, similar to mutations in other genes that regulate cell adhesion such as *hmr-1* (cadherin), *hmp-1* (alpha-catenin) and *hmp-2* (beta-catenin; Costa et al., 1998). To ascertain if the ventral enclosure defects were a consequence of earlier defects, dorsal intercalation was visualized in *ani-1* RNAi embryos. Dorsal intercalation in *ani-1* RNAi embryos was similar to control embryos, suggesting that *ani-1* is not required for earlier morphogenetic events (Table 4).

3.2.3 *ani-1* functions in parallel to the *rho-1* pathway

ani-1 may be required for ventral enclosure, but it is not clear how *ani-1* could regulate ventral epidermal cell migration or adhesion. Anillin is a regulator of actin-myosin contractility, suggesting that active myosin also may contribute to ventral enclosure. To determine if the *rho-1* pathway affects the lethality caused by *ani-1* RNAi, strains carrying mutations in genes known to regulate myosin contractility (*rho-1, mlc-4, let-502, mel-11, nmy-1, rhgf-2* and *let-502; mel-11*) were treated with *ani-1* RNAi, and monitored for embryonic lethality. The interaction between two genes was considered to be enhanced if the observed lethality exceeded predicted additive lethality rates, as

Table 4. *ani-1* is required for ventral enclosure.

Genotype	Dorsal Intercalation Defect	'Early' Ventral Enclosure Defect	'Late' Ventral Enclosure Defect
AJM-1::GFP/HMR-1::GFP; L4440 (n=10)	0	0	0
AJM-1::GFP/HMR-1::GFP; *ani-1* RNAi (n=19)	0	10	9

'Early' defects are when the ventral epidermal cells fail to meet at the midline and fail to adhere.

'Late' defects are when the ventral epidermal cells meet at the midline and appear to close, but show defects later in development (e.g. late rupture or larval Lpy Dpy; performed with D. Wernike).

determined by Chi-square analysis ($p < 0.05$). All of the mutant strains treated with *ani-1* RNAi showed enhanced embryonic lethality (Table 5 and Appendix 1). For example, *rho-1 (ok2418)/dpy-4*; *ani-1* RNAi displayed hatching rates of 13.9% vs. 73.4% for *rho-1 (ok2418)/dpy-4;* L4440 and 53.2% for *ani-1* RNAi, and the expected additive hatching rates were 26.6% (combined lethality; same logic applies to the rest of the RNAi experiments; Table 5 and Appendix 1).

Since *ani-1* RNAi sensitizes the early embryo for cytokinesis defects in combination with depletion of myosin and/or its regulators (Maddox et al., 2007), this could explain the enhancement between *ani-1* and *rho-1* or *mlc-4*. However, enhancement also was observed between *ani-1* RNAi and mutations in *nmy-1* and *rhgf-2*, genes that are zygotically required for elongation (Table 5 and Appendix 1). Mutations in these genes do no cause cytokinesis defects and the enhanced lethality with *ani-1* could arise from events during later stages of embryogenesis. Since *let-502* and *mel-11* are required both maternally for cytokinesis and maternally and zygotically for elongation, the enhanced lethality of *let-502* and *mel-11* could be due to increased cytokinetic defects or increased morphogenetic defects (Table 5 and Appendix 1). Enhancement of the double mutant, *let-502 (sb118); mel-11 (it26ts),* suggests that *ani-1* functions in parallel to the *let-502/mel-11* pathway for myosin contractility or *ani-1* regulates a different process altogether (e.g. stabilizing F-actin; Table 5 and Appendix 1).

3.2.4. *ani-1* depletion does not cause cytokinetic defects in epidermal cells

Since *ani-1* is maternally required for actin-myosin contractile events in the early embryo including cytokinesis, it is possible that *ani-1*'s ventral enclosure phenotypes

Table 5. *ani-1* is enhanced by regulators of myosin contractility.

Genotype	T°C	N2 on *ani-1* RNAi % Hatching	Mutant on L4440 % Hatching	Mutant on *ani-1* RNAi % Hatching	Effect*
rho-1(ok2418)/+	20	53.2	73.4	13.9	Enhancement
mlc-4(or253)/qC1	20	60.8	95.1	44	Enhancement
nmy-1(sb115)	20	56.7	89.9	19.9	Enhancement
let-502(sb118)	20	60	97.5	35	Enhancement
	25	63	0	0	Sterile
mel-11(it26)	15	53.1	13.8	0.9	Enhancement
	25	54	0	0	Sterile
let-502(sb118); mel-11(it26)	15	66	93.4	0	Enhancement
rhgf-2(sb100)	15	76.3	98.8	53.3	Enhancement

n > 300 per cross

* Significance tested by Chi-square analysis; *rho-1* ($p<0.05$); *mlc-4* ($p<0.05$); *mel-11* ($p<0.05$); *nmy-1* ($p<0.01$); *let-502* ($p<0.05$); *rhgf-2 I* ($p<0.05$); *let-502;mel-11* ($p<0.01$).

Data summarized from Appendix 1.

arise from cytokinesis defects in the epidermal cells. Interestingly, dorsal intercalation and ventral enclosure can still occur in embryos with fewer epidermal cells, although they show mild ventral enclosure phenotypes (Hardin et al., 2008). To determine if the ventral enclosure defects in *ani-1* RNAi embryos are from cytokinetic defects, the number of epidermal cells was counted in control and *ani-1* RNAi embryos. Control embryos should have 20 dorsal, 20 ventral and 20 seam cells. There were some difficulties in obtaining 3D projections that perfectly outlined every cell, and an average of 16 dorsal, 19 ventral cells, and 20 seam cells were counted for control AJM-1::GFP embryos. AJM-1::GFP; *ani-1* RNAi embryos that displayed ventral enclosure phenotypes had similar numbers of epidermal cells (19 dorsal, 19 ventral and 20 seam) vs. control embryos (performed with D. Wernike; Table 6). Therefore, the ventral enclosure phenotypes in *ani-1* depleted embryos likely are not due to cytokinetic defects in the epidermal cells.

3.2.5 ANI-1 is highly expressed in neuroblasts

ANI-1's localization was determined during mid-late embryogenesis to determine if it is consistent with its role in ventral enclosure. ANI-1::GFP (driven by the *pie-1* promoter), localizes to the contractile ring and cortex in the early embryo (Maddox et al., 2007). ANI-1 continues to localize to the contractile ring and cortex of dividing cells through the first half of embryogenesis, tapering off before dorsal intercalation (data not shown). Since the maternally-driven ANI-1 construct does not show zygotic expression, embryos of various stages were fixed and stained with ANI-1 antibodies. Similar to the GFP probe, antibodies revealed strong ANI-1 localization at contractile rings and cell boundaries in the early embryo (Figure 16). However, unlike the GFP probe, ANI-1 was

Table 6. *ani-1* depletion does not cause cytokinetic defects in epidermal cells.

Genotype	# Epidermal Dorsal Cells	# Epidermal Ventral Cells	# Epidermal Seam Cells
AJM-1::GFP or HMR-1::GFP	16 ± 2	19 ± 1	20 ± 1
AJM-1::GFP or HMR-1::GFP; *ani-1* RNAi	19 ± 1	19 ± 1	20 ± 1

Control (AJM-1::GFP or HMR-1::GFP) n = 21 for dorsal cells, n = 17 for ventral cells and n = 14 for seam cells

ani-1 RNAi (AJM-1::GFP or HMR-1::GFP) n = 20 for dorsal cells, n = 17 for ventral cells and n = 10 for seam cells

Embryos displaying ventral enclosure phenotypes (and not earlier) were counted (performed with D. Wernike).

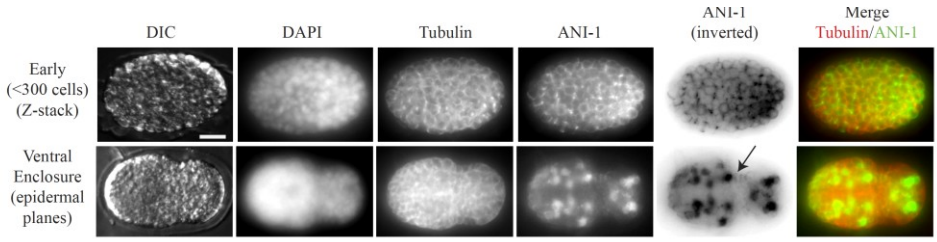

Figure 16. ANI-1 localizes to cell boundaries and contractile rings of dividing cells during embryogenesis. Z-stack projections of fluorescent images of immunostained N2 embryos showing ANI-1 localization at cleavage furrows and cell boundaries in an early embryo (panels on top). ANI-1 appears to localize in dividing neuroblasts during ventral enclosure. Shown are DIC, DAPI (for DNA), Tubulin and ANI-1 images. Merged images with Tubulin in red and ANI-1 in green are also shown. The arrow points to cell boundaries in cells near the ventral surface. Scale bar is 10 μm.

enriched in dividing cells underneath the epidermis, likely neuroblasts (Figure 16). Confocal images of AJM-1::GFP embryos co-stained for GFP and ANI-1 during ventral enclosure verified that ANI-1 does not localize within epidermal cells (based on z planes of 0.2 μm thickness; Figure 17). Therefore, although *ani-1* depletion causes ventral enclosure phenotypes, ANI-1 is not expressed in ventral epidermal cells suggesting that *ani-1* functions in a non-autonomous manner. Other genes that function in neuroblasts, such as *vab-1* and *vab-2*, are also required for ventral enclosure likely because the neuroblasts act as a substrate for epidermal cell migration (Chin-Sang et al., 1999; Chin-Sang et al., 2002).

To determine if ANI-1 is expressed in specific subsets of neuroblast cells, attempts were made to co-stain ANI-1 with VAB-1 and VAB-2/EFN-1. VAB-1 is expressed in anterior neuroblasts, while EFN-1 is expressed in cells in the middle of the embryo. Strains over-expressing VAB-1 or VAB-2 were fixed and stained with antibodies against ANI-1 and VAB-1 or VAB-2 (Courtesy of I. Chin-Sang, Queen's University). Since all antibodies were generated in rabbits, goat anti-rabbit Fab fragments were used to change the identity of one of the antisera (e.g. ANI-1 or VAB-1 or VAB-2) to goat. However, tests with control embryos revealed that the Fab fragments could not convert 100% of the ANI-1 antisera to goat, making it difficult to properly co-stain ANI-1 with VAB-1 or VAB-2. Studies are currently underway to co-stain ANI-1 in embryos expressing other markers for neuroblast cells.

3.2.6 Tissue specific knockdown of *ani-1*

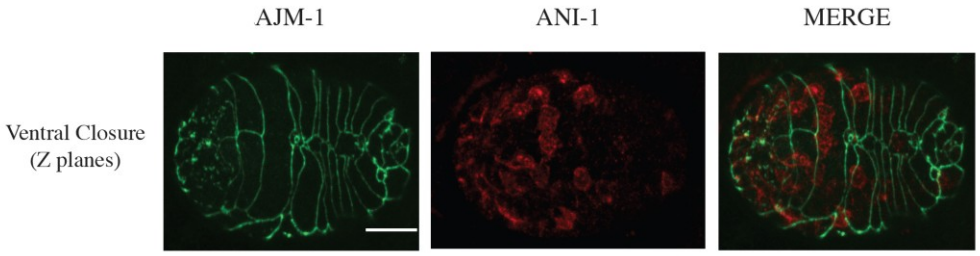

Figure 17. ANI-1 is expressed in the neuroblasts underlying the ventral epidermal cells. Confocal images show the localization of ANI-1 and AJM-1 during late ventral enclosure in AJM-1::GFP-expressing, fixed embryos. ANI-1 (red) appears to localize to the underlying neuroblasts as opposed to the epidermal cells, which are outlined in green. Scale bar is 10 μm.

ani-1 may be required non-autonomously in the neuroblasts to regulate ventral enclosure. To test *ani-1*'s requirement in the epidermal cells, a mosaic analysis was performed using RNAi-resistant worms carrying rescue constructs under the control of an epidermal cell-specific promoter or a muscle cell-specific promoter (as a control). The *rde-1 (nr222)* strain is 'rescued' with a wild-type allele in the epidermal cells, making only this tissue permeable to RNAi treatments. Therefore, any phenotypes that arise after RNAi support a requirement for that gene in epidermal cells. As a control, *rde-1 (nr350)* was used, which is 'rescued' with a wild-type allele in muscle tissue. Any gene that is required in the epidermal cells, but not in the muscle tissue should only show lethality with the *nr222* allele, but not with the *nr350* allele after RNAi. To test the strains, both were treated with *rho-1* RNAi, which is known to function in the epidermal cells, but not in the muscle. Typically, *rho-1* RNAi is used a control for testing the efficacy of RNAi since it quickly depletes endogenous *rho-1* in N2 embryos, and shows 100% lethality within 24 hours. Unfortunately, both strains showed 100% hatching, suggesting a problem with the *nr222* strain. Therefore, *ani-1* was not tested using these strains. Current studies will attempt to perform rescue experiments by expressing *ani-1* under the control of tissue-specific promoters (to be performed by D. Wernike).

3.2.7 Myosin Contractility May Influence Ventral Enclosure

ani-1 functions non-autonomously to regulate ventral enclosure, and is expressed in dividing neuroblasts. It is not clear how the neuroblasts regulate the migration of the overlying ventral epidermal cells. Previous studies suggest that ephrin and semaphorin signaling pathways could provide chemical guidance cues, but there are other pathways

and/or mechanisms that remain to be determined (Ghenea et al. 2005; Ikegami et al. 2012). We hypothesize that *ani-1* could be required for the division and/or stiffness of neuroblasts, which could alter their ability to regulate epidermal cell migration in a mechanical manner. To help test this, myosin contractility was altered in the epidermal cells to determine how they influence the ventral enclosure phenotypes caused by *ani-1* RNAi. Embryos with different contractile backgrounds (*let-502 (sb118), mel-11 (it26)* and *nmy-1 (sb115))* were treated with *ani-1* RNAi and imaged by time lapse. Embryos were placed into several categories based on their mutant phenotypes. 'Early' describes embryos that did not reach ventral enclosure, 'early rupture' are embryos that failed ventral enclosure and ruptured prior to undergoing extensive elongation (until the 1.5-fold stage), 'late rupture' are embryos that ruptured during elongation (after the 1.5-fold stage) and 'elongation' phenotypes describe embryos that did not rupture, but failed to complete elongation (Table 7). The majority of *ani-1* RNAi embryos arrested early (likely due to meiotic and cytokinesis defects), with a relatively even distribution of embryos in the remaining categories (Table 7). *let-502 (sb118)*; *ani-1* RNAi embryos had an increased number of early and elongation phenotypes and a decrease in the proportion of ventral enclosure defects vs. *ani-1* RNAi (Table 7 and Figure 18). The enhanced percentage of early phenotypes likely reflects *let-502*'s maternal requirement for cytokinesis, while the enhanced elongation phenotypes reflects *let-502*'s maternal and zygotic requirement for elongation. The decrease in ventral enclosure phenotypes could be explained by weakened pressure on the embryo from decreased myosin contractility in the epidermal cells. Interestingly, *nmy-1 (sb115); ani-1* RNAi embryos showed an

Table 7. Myosin Contractility May Influence Ventral Enclosure

Genotype	Early	Early VE Rupture*	Late VE Rupture*	Elongation Phenotypes **
N2 (wt)	0	0	0	0
ani-1 RNAi	51.6	22.6	9.7	16.1
let-502(sb118ts)	52.2	-	-	47.8
let-502(sb118ts); ani-1 RNAi	65.9	7.3	-	26.8
nmy-1(sb115)	10.1	-	-	89.9
nmy-1(sb115); ani-1 RNAi	38.7	11.5	38.7	11.5
mel-11(it26ts)	8.3	8.3	83.3	-
mel-11(it26ts); ani-1 RNAi	41.2	58.8	-	-

n ≥30 embryos, except for *mel-11(it26ts); ani-1* RNAi where n=15

*Early VE (ventral enclosure) rupture is defined as ventral enclosure rupture up to and including the 1.5-fold stage of elongation, and late VE rupture is defined as rupture after the 1.5-fold stage of elongation.

**Elongation phenotypes include embryos arrested at different stages of elongation without rupture.

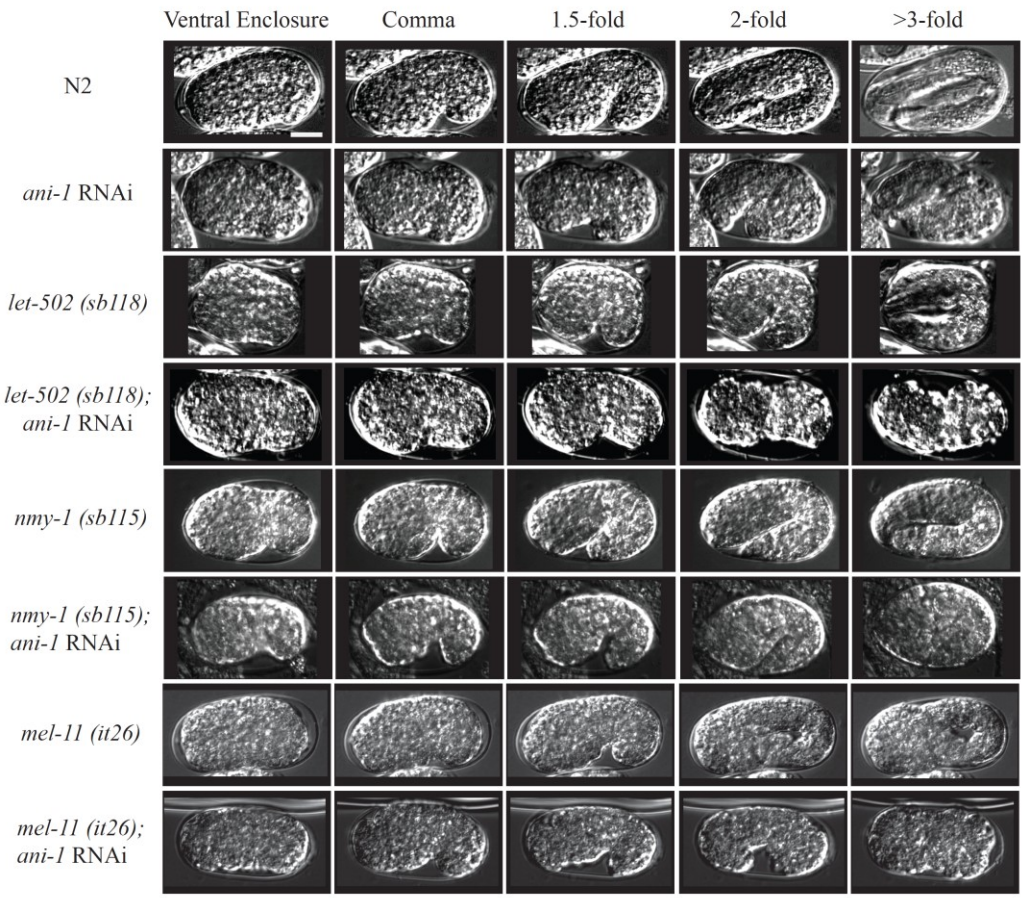

Figure 18. *ani-1*'s ventral enclosure phenotypes are enhanced or suppressed by regulators of myosin contractility. DIC images from time lapse movies of N2, *ani-1* RNAi, *let-502 (sb118), let-502 (sb118*); *ani-1* RNAi, *nmy-1 (sb115), nmy-1 (sb115); ani-1* RNAi*, mel-11 (it26)* and *mel-11 (it26); ani-1* RNAi from ventral enclosure to past the 3-fold stage of elongation. All imaging was done at room temperature (22°C). Scale bar is 10 μm.

increase in late rupture phenotypes vs. *ani-1* RNAi (Table 7 and Figure 18). Since *nmy-1* is partially redundant with *nmy-2* for elongation (Piekny et al., 2003), these embryos likely have more contractility in their epidermal cells and thus more pressure may be exerted from these cells in comparison to *let-502* mutants, but not as much as wild-type embryos. Lastly, *mel-11* embryos tend to rupture during elongation, likely due to hypercontracting epidermal cells, which exert too much pressure on the internal contents of the embryo. The shift to early rupture phenotypes after *ani-1* depletion suggests that these embryos are sensitized to pressure changes (Table 7 and Figure 18). These data support a mechanical role for *ani-1* (and neuroblasts) in ventral enclosure.

Chapter 4. Discussion

The epidermis of the developing *C. elegans* embryo undergoes several morphogenetic events including ventral enclosure to enclose the embryo in a layer of epidermal tissue, and elongation to increase the length of the embryo up to 4-fold. Elongation occurs due to actomyosin-mediated cell shape changes, yet the upstream regulator RhoA had not been shown to be required for this event. Ventral enclosure also requires changes in the actin cytoskeleton to drive migration and cell adhesion. Migration of the ventral epidermal cells is non-autonomously regulated by neuroblasts, however, the mechanism(s) by which they do this is poorly understood. Identifying novel regulators of epidermal morphogenesis in *C. elegans* can shed light on how metazoan tissues form in vivo. My thesis confirms that *C. elegans* RhoA (*rho-1)* as an upstream regulator of elongation and describes a novel non-autonomous role for *C. elegans* anillin (*ani-1)* in ventral enclosure.

4.1 *rho-1* is required for elongation

Elongation occurs due to the concerted activity of Rho-dependent kinase (LET-502), which positively regulates nonmuscle myosin activity and myosin phosphatase regulatory subunit (MEL-11), which down regulates myosin activity via myosin phosphatase. High levels of LET-502 in the lateral epidermal cells drive elongation, while high levels of MEL-11 in the dorsal and ventral cells ensure they follow passively (Wissmann et al. 1997; Piekny et al., 2000). Since LET-502 is a predicted effector for RHO-1, it is likely that *rho-1* also is required for elongation, yet until recently there were no *rho-1* alleles (Wissmann et al. 1997; Piekny et al. 2000; Diogon et al., 2007). Using a

zygotic null allele created by the Knockout Consortium, I found that *rho-1* is required for elongation. The *rho-1* phenotype, two-fold arrest, is slightly later vs. strong *let-502* alleles, which cause arrest at the comma to1.5-fold stage. *rho-1* may be required both maternally and zygotically, similar to *let-502*, and the shift to later phenotypes reflects the maternal vs. zygotic contribution of *rho-1* to elongation. In support of this, RHO-1::GFP, which is driven by the maternal promoter *pie-1*, localizes to epidermal cell boundaries throughout elongation. This suggests that maternal RHO-1 is very stable, and may be sufficient to drive early elongation, but the embryo needs a boost of zygotic expression to complete elongation.

rho-1 functions in the elongation pathway based on its genetic interactions with components of the pathway that regulate nonmuscle myosin activity, including *mlc-4* (nonmuscle myosin regulatory light chain), *let-502* (Rho kinase)*, mel-11* (myosin phosphatase regulatory subunit) and *rhgf-2* (RhoGEF). There was no genetic interaction between zygotic null alleles for both *rho-1* and *mlc-4*, suggesting that they function in the same pathway. However, embryos (or lack thereof) from *let-502 (sb118); rho-1 /+* hermaphrodites showed enhancement, which could be due to the decreased levels of maternal *rho-1* in these embryos. Elongation requires both maternal and zygotic *let-502* (Piekny et al., 2000) and similarly both maternal and zygotic *rho-1* could be required for elongation (and other contractile events). This makes the interpretation of genetic crosses using hypomorphic *let-502* alleles complicated. Moreover, ovulation and germ cell proliferation depend on *let-502*, so lowering its levels of could disrupt and/or sensitize these processes within the hermaphrodite. Further support for *rho-1* in the elongation pathway is from the suppression of *mel-11* embryonic lethality by the *rho-1* mutant.

Mutations in *let-502* and *mel-11* dominantly suppress one another and an upstream regulator of *let-502* should similarly suppress *mel-11*. Removal of MEL-11 (a negative regulator of nonmuscle myosin) causes epidermal cells to hypercontract, and removing RHO-1 (a positive regulator of contraction via LET-502) likely alleviates the hypercontraction. Furthermore, although the number was low, some embryos hatched and displayed *rho-1* phenotypes (larval Lpy Dpy), which is expected if *rho-1* is an essential gene. Therefore, unlike *let-502*, *rho-1* is essential for elongation and could regulate additional proteins.

RHGF-2 is the predicted RhoGEF and activator of RHO-1 during elongation (Lin et al. 2012). The weak enhancement observed between alleles of *rhgf-2* and *rho-1* suggests that they function in separate pathways. However, strong enhancement between *rhgf-2* and *fem-2* (functions in a parallel pathway to *let-502/mel-11*) implies that *rhgf-2* and *let-502* function in the same pathway (P.E. Mains, personal communication). Furthermore, the phenotype of the double mutant is the same as each on its own, supporting that they regulate the same process. Taking these findings into account, we hypothesize that *rho-1* and *rhgf-2* function in the same pathway.

4.2 *ani-1* is non-autonomously required for ventral enclosure during *C. elegans* embryonic development

Anillin is a scaffold for actin and myosin, and helps organize actin-myosin contractility during cytokinesis and meiotic polar body extrusion (Maddox et al. 2005; Maddox et al. 2007; Dorn et al. 2010; Tse et al., 2011). Morphogenetic phenotypes were described for *ani-1* RNAi in adult worms (Maddox et al. 2005), but additional embryonic

and/or larval phenotypes have not been reported. My data supports a role for *ani-1* in ventral enclosure. Live imaging of AJM-1::GFP; *ani-1* RNAi embryos revealed that although they appeared to have undergone dorsal intercalation properly, they displayed ventral enclosure phenotypes. Another regulator of cytokinesis, *zen-4*, causes morphogenetic defects, and these embryos had fewer epidermal cells vs. wt embryos. However, even with fewer cells, ventral epidermal cells migrated with similar dynamics to wt embryos, but adhesion was affected, likely due to uneven sealing at the midline (Hardin et al., 2008). This suggests that the *ani-1* phenotypes are not simply a consequence of too few ventral epidermal cells. Indeed, co-staining fixed embryos undergoing ventral enclosure with ANI-1 antibodies and AJM-1 (adherens junction marker that outlines the boundary of epidermal cells) revealed that ANI-1 was not strongly expressed in the epidermal cells and confocal images imply that ANI-1 is expressed in the underlying neuroblast cells. Therefore, *ani-1* may function non-autonomously to regulate ventral enclosure. ANI-1 localized to cleavage furrows in the dividing neuroblasts, and remained at the boundaries of some cells, suggesting that *ani-1* could be required for their division, similar to cells in other metazoans (Piekny and Maddox, 2010). Since neuroblasts function as a substrate for the migrating ventral epidermal cells (George et al., 1998; Chin-Sang et al., 1999; Chin-Sang et al., 2002; Harrington et al., 2002), cytokinesis defects could alter their organization and stiffness, so that they no longer function as an effective substrate.

Two categories of ventral enclosure phenotypes were observed in *ani-1*-depleted embryos. 'Early' describes the inability of ventral epidermal cells to reach the ventral midline, leaving a gap that ruptures by the comma stage. In embryos with the 'late'

phenotype, ventral epidermal cells reached the midline, but failed to adhere correctly and ruptured during elongation, or hatched, but displayed abnormal body morphologies (Lpy Dpy). As mentioned above, ANI-1 is zygotically expressed in dividing neuroblasts, suggesting that *ani-1*'s affect on ventral enclosure is non-autonomous. The relatively equal distribution of both early and late ventral enclosure phenotypes suggests that there could be different threshold requirements for *ani-1* in neuroblasts. For example, strong depletion of *ani-1* could cause neuroblast cytokinesis defects, and the decreased number of cells could impede the proper migration of ventral epidermal cells and cause the 'early' phenotype. Weak depletion of *ani-1* could still permit the appropriate number of neuroblasts to form, but could weaken their actin-myosin cytoskeleton and be less stiff of a substrate for the overlying epidermal cells. The migration of ventral epidermal cells could still occur, but may not adhere properly due to misalignment, causing the 'late' phenotype. Genes known to regulate adhesion, which include *hmp-1* (alpha catenin), *hmp-2* (beta catenin) and *hmr-1* (e-cadherin), display abnormal body morphology phenotypes consistent with 'late' *ani-1* phenotypes (Chisholm and Hardin, 2005). A recent study by Goldbach et al. (2010) showed that overexpression of E-cadherin in *Drosophila* spermatids suppresses cytokinesis defects in *ani-1*-depleted cells. A colleague of mine, Denise Wernike, investigated the potential genetic interactions between *ani-1* and adhesion genes and found that over-expression of α-catenin, *hmp-1*, can suppress the *ani-1* phenotype and vice versa (*i.e.* over-expression of *ani-1* can suppress loss of *hmp-1*). A possible explanation for this finding is that strengthening cell adhesion between neighboring cells at the ventral midline may make up for the loss of *ani-1* and prevent

future rupturing. I propose a model where neuroblasts act as a substrate for the overlying ventral epidermal cells by providing mechanical support.

Despite the observation that little ANI-1 was observed in the ventral epidermal cells by immunostaining, it is still possible that *ani-1* is required in the ventral epidermal cells. Short, branched F-actin filaments mediate migration of the ventral cells via the activities of Rac (*ced-10*), Arp2/3 (*arx-2/3*), WAVE/SCAR regulators (*gex-2* and *gex-3*) and WASP (*wsp-1*; Williams-Masson et al., 1997; Soto et al., 2002; Patel et al., 2008). However, there could be a role for long, unbranched F-actin and active myosin. In higher eukaryotes, migration often requires the combination of both systems, with the force-generating component coming from the contraction of stress fibres in the rear of the cell, which are adhered to underlying substrate. Another aspect of ventral enclosure is the closing of the ventral pocket, which is hypothesized to occur by a purse-string mechanism (Chisholm and Hardin, 2005). Presumably, this type of closure would require active myosin, and *ani-1* could crosslink actin-myosin contractility to promote this event.

4.3 Altering myosin contractility alters ventral enclosure defects in *ani-1* RNAi embryos

The non-autonomous regulation of epidermal tissue formation is not well understood. Previous studies showed that ephrin signaling is required for *C. elegans* ventral enclosure, and these components (e.g. VAB-1 and VAB-2) are expressed within neuroblasts (Chin-Sang et al. 1999). However, these studies also revealed that multiple mechanisms likely contribute to ventral enclosure, which are not known. My data revealed that *ani-1*, which encodes a scaffold for F-actin and active myosin, and regulates

actin-myosin contractility in the early embryo, is non-autonomously required for ventral enclosure. Since ANI-1 is expressed in the neuroblasts and could regulate their actin-myosin cytoskeleton for cytokinesis or for cortical stiffness, I propose that neuroblasts could mechanically regulate the migration of overlying ventral epidermal cells. To help test this, we determined how changing cortical tension affected *ani-1*'s ventral enclosure phenotypes. Not surprisingly, enhancement of embryonic lethality was observed with all strains carrying mutations in components of the elongation pathway that regulate myosin contractility [*rho-1, mlc-4, let-502, mel-11*, *rhgf-2* and *nmy-1* (nonmuscle myosin heavy chain)]. Previous studies had shown that *ani-1* RNAi sensitizes embryos to cytokinesis defects when combined with mutations in other contractile ring components including myosin (*nmy-2* and *mlc-4*) and *let-502* (Rho kinase; Maddox et al., 2005; Maddox et al., 2007). However, imaging embryos that did not show these early phenotypes revealed shifts in ventral enclosure defects, depending on the elongation mutant. For example, mutations with decreased contractility e.g. in *let-502,* displayed a lower proportion of ventral enclosure defects after *ani-1* RNAi. Mutations in *nmy-1* display intermediate levels of contractility (it is partially redundant with *nmy-2*) and these embryos shifted to a higher proportion of late ventral enclosure defects after *ani-1* RNAi. Mutations in *mel-11* likely cause hypercontractility and embryos shifted to a higher proportion of early ventral enclosure defects after *ani-1* RNAi. These shifts in phenotypes reflect the roles of these genes in regulating myosin activity. Loss of LET-502 likely causes lower levels of myosin contractility and failed elongation due to lack of epidermal cell shape changes. This could decrease tension across cells and alleviate rupturing despite the inefficient migration or adhesion of ventral epidermal cells (Wissmann et al., 1997; Wissmann et al.,

1999; Piekny et al., 2000; Piekny et al., 2003; Diogon et al., 2007; Gally et al., 2009). However, the suppression could indicate a unique requirement for myosin contractility in the ventral epidermal cells, and although the migratory defects of the ventral epidermal cells are rescued, it would be interesting to determine if they migrate with the same velocity as wt cells. Loss of MEL-11 causes higher levels of myosin contractility and rupture of the embryo likely due to hyper-contraction of the epidermal cells and increased tension across cells (Wissmann et al., 1997; Wissmann et al., 1999; Piekny et al., 2000; Piekny et al., 2003; Diogon et al., 2007; Gally et al., 2009).

In conclusion, this work helps shed light on how tissues form in vivo. Cell shape changes and migration are regulated by the actin-myosin cytoskeleton, and are crucial for the development of all metazoans. Furthermore, similar events drive metastasis and the advancement of cancers. This thesis describes a novel role for *C. elegans* anillin (*ani-1*) in the non-autonomous regulation of ventral enclosure, which is a key step in the formation of epidermal tissue during *C. elegans* development. ANI-1 is highly expressed in dividing neuroblasts and since anillin regulates cytokinesis in other metazoans, *ani-1* depletion could decrease the number of neuroblasts and impede the migration of overlying ventral epidermal cells. My data supports a mechanical model for regulating cell migration in vivo, which could improve our understanding of metazoan tissue formation. Furthermore, anillin is over-expressed in cancerous tumors in comparison to healthy tissues (Hall et al. 2005). Although anillin is likely upregulated to maintain the high proliferation rate of cancer cells, it also may be increased to promote higher cell motility and increase the chances of metastasis.

Appendix

Appendix 1

A

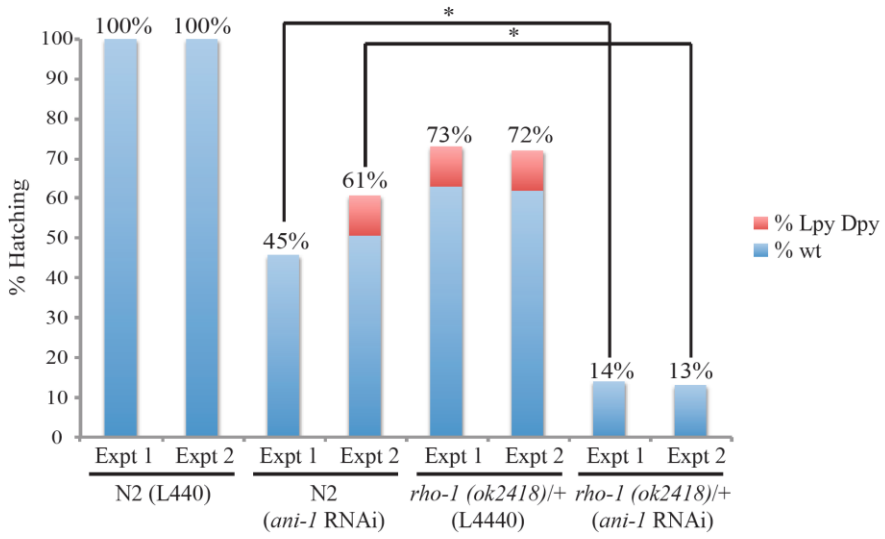

B

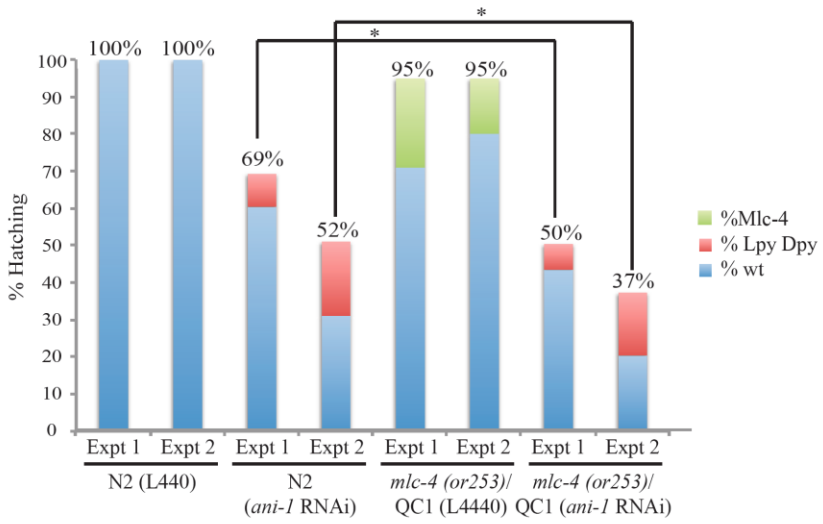

C

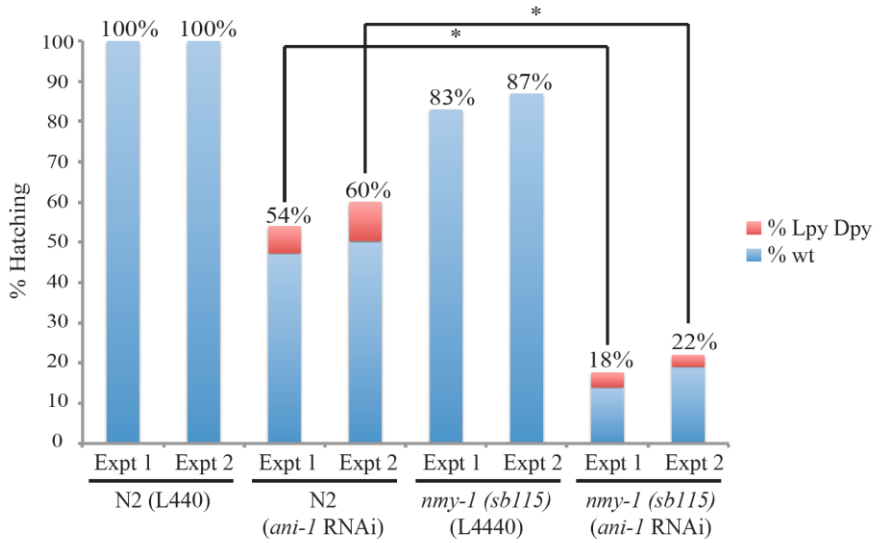
% Hatching
100%
100%
54%
60%
83%
87%
18%
22%
*
*
% Lpy Dpy
% wt
Expt 1
Expt 2
N2 (L440)
N2
(ani-1 RNAi)
nmy-1 (sb115)
(L4440)
nmy-1 (sb115)
(ani-1 RNAi)

D

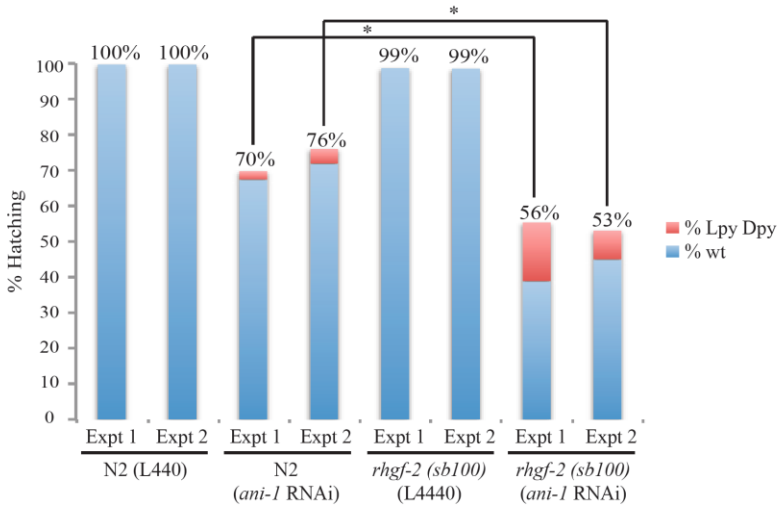
% Hatching
100%
100%
70%
76%
99%
99%
56%
53%
*
*
% Lpy Dpy
% wt
Expt 1
Expt 2
N2 (L440)
N2
(ani-1 RNAi)
rhgf-2 (sb100)
(L4440)
rhgf-2 (sb100)
(ani-1 RNAi)

E

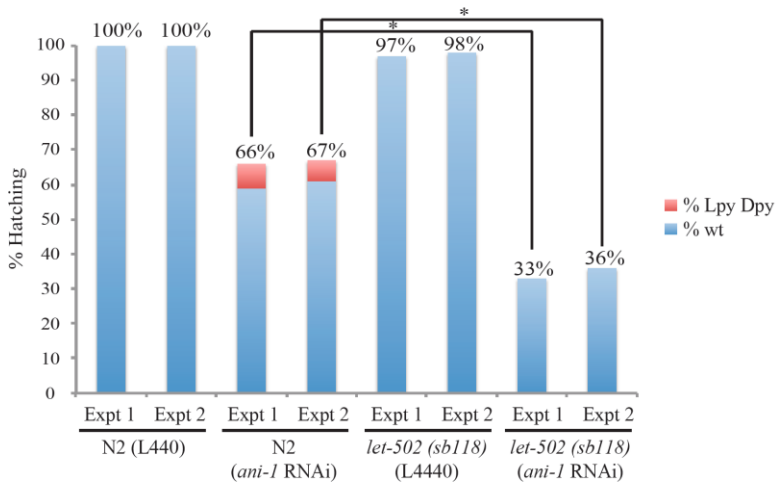
100%
100%
66%
67%
97%
98%
33%
36%
*
*
% Hatching
100
90
80
70
60
50
40
30
20
10
0
Expt 1
Expt 2
N2 (L440)
N2
(ani-1 RNAi)
let-502 (sb118)
(L4440)
let-502 (sb118)
(ani-1 RNAi)
% Lpy Dpy
% wt

F

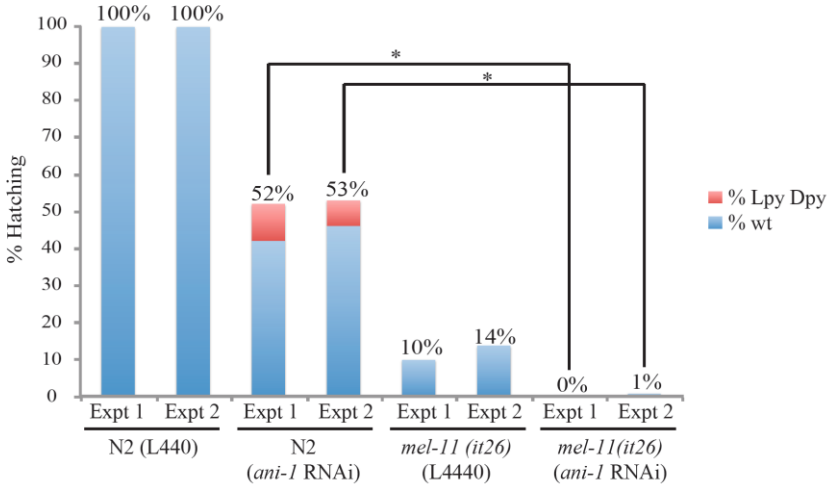
100%
100%
52%
53%
10%
14%
0%
1%
*
*
% Hatching
100
90
80
70
60
50
40
30
20
10
0
Expt 1
Expt 2
N2 (L440)
N2
(ani-1 RNAi)
mel-11 (it26)
(L4440)
mel-11(it26)
(ani-1 RNAi)
% Lpy Dpy
% wt

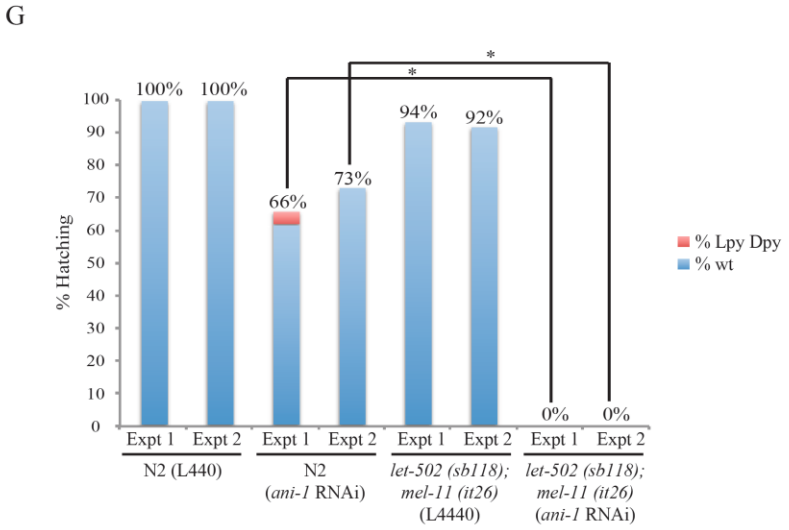

Figure 16. *ani-1* RNAi embryonic lethality is enhanced by mutations in genes that regulate myosin contractility. Graphs shows the percent hatching for two sets of *ani-1* RNAi experiments for different mutant alleles of genes in the *rho-1*/elongation pathway. Chi-square tests were used to determine statistical significance. A) Shows hatching rates (blue) and Lpy Dpy larva (red) of *rho-1 (ok2418)/+* with or without *ani-1* RNAi, The asterix indicates $p < 0.05$. B) Shows hatching rates (blue), Lpy Dpy larva (red) and Mlc-4 larva (green) of *mlc-4 (or253)/qCI* with or without *ani-1* RNAi, The asterix indicates $p < 0.05$. C) Shows hatching rates (blue) and Lpy Dpy larva (red) of *nmy-1 (sb115)* with or without *ani-1* RNAi, The asterix indicates $p < 0.01$. D) Shows hatching rates (blue) and Lpy Dpy larva (red) of *rhgf-2 (sb100)* with or without *ani-1* RNAi, The asterix indicates $p < 0.05$. E) Shows hatching rates (blue) and Lpy Dpy larva (red) of *let-502 (sb118)* with or without *ani-1* RNAi, The asterix indicates $p < 0.05$. F) Shows hatching rates (blue) and Lpy Dpy larva (red) of *mel-11 (it26)* with or without *ani-1* RNAi, The asterix indicates $p < 0.05$ G) Shows hatching rates (blue) and Lpy Dpy larva (red) of *let-502 (sb118); mel-11 (it26)* with or without *ani-1* RNAi, The asterix indicates $p < 0.01$.

References

Abmayr, S. M. and Pavlath, G. K. **Myoblast fusion: lessons from flies and mice.** Development. 2012, 139: 641-56.

Ahuja, R., Pinyol, R., Reichenbach, N., Custer, L., Klingensmith, J., Kessels, M. M. and Qualmann, B. **Cordon-bleu is an actin nucleation factor and controls neuronal morphology**. Cell. 2007, 131: 337-350.

Alberts, A. S. **Identification of a carboxyl-terminal diaphanous-related formin homology protein autoregulatory domain.** J. Biol. Chem. 2001, 276: 2824-2830.

Amano, M., Ito, M., Kimura, K., Fukata, Y., Chihara, K., Nakano, T., Matsuura, Y. and Kaibuchi, K. **Phosphorylation and activation of myosin by Rho-associated kinase (Rho-kinase)**. J. Biol. Chem. 1996, 271: 20246-20249.

Anderson, D. C., Gill, J. S., Cinalli, R. M. and Nance, J. **Polarization of the C. elegans embryo by RhoGAP-mediated exclusion of PAR-6 from cell contacts.** Science. 2008, 320: 1771-1774.

Baum, B. and Georgiou, M. **Dynamics of adherens junctions in epithelial establishment, maintenance, and remodeling.** J. Cell Biol. 2011, 192: 907-917.

Bement, W. M., Forscher, P. and Mooseker, M. S. **A novel cytoskeletal structure involved in purse string wound closure and cell polarity maintenance.** J. Cell Biol. 1993, 121: 565-78.

Bement, W. M., Benink, H. A. and von Dassow, G. **A microtubule-dependent zone of active RhoA during cleavage plane specification.** J. Cell Biol. 2005, 170: 91-101.

Bompard, G., Sharp, S. J., Freiss, G. and Machesky, L. M. **Involvement of Rac in actin cytoskeleton rearrangements induced by MIM-B.** J. Cell Sci. 2005, 118: 5393-5403.

Bray, D. and White, J. G. **Cortical flow in animal cells.** Science. 1988, 239: 883-888.

Brenner. S. **The genetics of Caenorhabditis elegans.** Genetics. 1974, 77: 71-94.

Chin-Sang, I. D., George, S. E., Ding, M., Moseley, S. L., Lynch, A. S. and Chisholm, A. D. **The ephrin VAB-2/EFN-1 functions in neuronal signaling to regulate epidermal morphogenesis in C.elegans.** Cell. 1999, 99: 781-790.

Chin-Sang, I. D. and Chisholm A. D. **Form of the worm: genetics of epidermal morphogenesis in C.elegans.** Trends Genet. 2000, 16: 544-551.

Chin-Sang, I. D., Moseley, S. L., Ding, M., Harrington, R. J., George, S. E. and Chisholm, A. D. **The divergent C. elegans ephrin EFN-4 functions in embryonic morphogenesis in a pathway independent of the VAB-1 Eph receptor.** Development. 2002, 129: 5499-5510.

C.elegans Sequencing Consortium. **Genome sequence of the nematode C. elegans: a platform for investigating biology.** Science. 1998, 282: 2012-2018.

Chisholm, A. D. and Hardin, J. **Epidermal morphogenesis**. WormBook. 2005, the online review of C. elegans biology: 1-22.

Costa, M., Raich, W., Agbunag, C., Leung, B., Hardin, J. and Priess, J. R. **A putative catenincadherin system mediates morphogenesis of the Caenorhabiditis elegans embryo.** J. Cell Biol. 1998, 141: 297-308.

Craig, R., Smith, R. and Kendrick-Jones, J. **Light-chain phosphorylation controls the conformation of vertebrate non-muscle and smooth muscle myosin molecules.** Nature. 1983, 302: 436-439.

Curran, S. P., Wu, X., Riedel, C. G. and Ruvkun, G. **A soma-to-germline transformation in long-lived Caenorhabditis elegans mutants.** Nature. 2009, 459: 1079-1084.

D'Avino, P. P., Takeda, T., Capalbo, L., Zhang, W., Lilley, K. S., Laue, E. D. and Glover, D. M. **Interaction between Anillin and RacGAP50C connects the actomyosin contractile ring with spindle microtubules at the cell division site.** J. Cell Sci. 2008, 121: 1151-1158.

Diogon, M., Wissler, F., Quintin, S., Nagamatsu, Y., Sookhareea, S., Landmann, F., Hutter, H., Vitale, N. and Labouesse, M. **The RhoGAP RGA-2 and LET-502/ROCK achieve a balance of actomyosin-dependent forces in C. elegans epidermis to control morphogenesis.** Development. 2007, 134: 2469-2479.

Dorn, J. F., Zhang, L., Paradis, V., Edoh-Bedi, D., Jusu, S., Maddox, P. S. and Maddox, A. S. **Actomyosin tube formation in polar body cytokinesis requires Anillin in C. elegans.** Curr. Biol. 2010, 20: 2046-2051.

Dvorsky, R. and Ahmadian, M. R**. Always look on the bright site of Rho: structural implications for a conserved intermolecular interface.** EMBO. 2004, 12: 1130-1136.

Evangelista, M., Pruyne, D., Amberg, D. C., Boone, C. and Bretscher, A. **Formins direct Arp2/3-independent actin filament assembly to polarize cell growth in yeast.** Nat. Cell Biol. 2002, 4: 260-269.

Field, C. M. and Alberts, B. M. **Anillin, a contractile ring protein that cycles from the nucleus to the cell cortex.** J. Cell Biol. 1995, 131: 165-178.

Field, C. M., Coughlin, M., Doberstein, S., Marty, T. and Sullivan, W. **Characterization of anillin mutants reveals essential roles in septin localization and plasma membrane integrity.** Development. 2005, 132: 2849-2860.

Fraser, A. G., Kamath, R. S., Zipperlen, P., Martinez-Campos, M., Sohrmann, M. and Ahringer, J. **Functional genomic analysis of C. elegans chromosome I by systematic RNA interference.** Nature. 2000, 408: 325-330.

Frenette, P., Haines, E., Loloyan, M., Kinal, M., Pakarian, P. and Piekny, A. **An anillin-Ect2 complex stabilizes central spindle microtubules at the cortex during cytokinesis.** PLoS One. 2012, 7: e34888.

Gally, C., Wissler, F., Zahreddine, H., Quintin, S., Landmann, F. and Labouesse, M. **Myosin II regulation during C. elegans embryonic elongation: LET-502/ROCK, MRCK-1 and PAK-1, three kinases with different roles.** Development. 2009, 136: 3109-3119.

George, S. E., Simokat, K., Hardin, J. and Chisholm, A. D. **The VAB-1 Eph receptor tyrosine kinase functions in neural and epithelial morphogenesis in C. elegans.** Cell. 1998, 92: 633-643.

Ghenea, S., Boudreau, J. R., Langue, N. P. and Chin-Sang, I. D. **The VAB-1 Eph receptor tyrosine kinase and SAX-3/Robo neuronal receptors function together during C. elegans embryonic morphogenesis.** Development. 2005, 132: 3679-3690.

Glotzer, M. **Animal cell cytokinesis.** Annu. Rev. Cell Dev. Biol. 2001, 17: 351-86.

Goldbach, P., Wong, R., Beise, N., Sarpal, R., Trimble, W. S. and Brill, J. A.

Stabilization of the actomyosin ring enables spermatocyte cytokinesis in Drosophila. Mol. Biol. Cell. 2010, 21: 1482-1493.

Goode, B. L. and Eck, M. J. **Mechanism and function of formins in the control of actin assembly.** Annu. Rev. Biochem. 2007, 76: 593-627.

Gregory, S. L., Ebrahimi, S., Milverton, J., Jones, W. M., Bejsovec, A. and Saint, R. **Cell division requires a direct link between microtubule-bound RacGAP and Anillin in the contractile ring.** Curr. Biol. 2008, 18: 25-29.

Hall, A. **Rho GTPases and the actin cytoskeleton.** Science. 1998, 279: 509-514.

Hall, P. A., Todd, C. B., Hyland, P. L., McDade, S. S., Grabsch, H., Dattani, M., Hillan, K. J. and Russell, S. E. **The Septin-binding protein anillin is overexpressed in diverse human tumors.** Clin Cancer Res. 2005, 11: 6780-6786.

Hardin, J., King, R., Thomas-Virnig, C., Raich, W.B. **Zygotic loss of ZEN-4/MKLP1 results in disruption of epidermal morphogenesis in the C. elegans embryo.** Dev Dyn. 2008, 237: 830-836.

Harrell, J. R. and Goldstein, B. **Internalization of multiple cells during C. elegans gastrulation depends on common cytoskeletal mechanisms but different cell polarity and cell fate regulators.** Dev. Biol. 2010, 341: 5-19.

Harrington, R. J., Gutch, M. J., Hengartner, M. O., Tonks, N. K. and Chisholm, A. D. **The C.elegans LAR-like receptor tyrosine phosphatase PTP-3 and the VAB-1 Eph receptor tyrosine kinase have partly redundant functions in morphogenesis.** Development. 2002, 129: 2141-2153.

Heid, P. J., Raich, W. B., Smith, R., Mohler, M. A., Simokat, K., Gendreau, S. B., Rothman, J. H. and Hardin, J. **The zinc finger protein DIE-1 is required for late events during epithelial cell rearrangement in C. elegans.** Dev. Biol. 2001, 236: 165-180.

Hickson, G. R. and O'Farrell, P. H. **Rho-dependent control of anillin behavior during cytokinesis.** J. Cell Biol. 2008, 180: 285-294.

Ikegami, R., Simokat, K., Zheng, H., Brown, L., Garriga, G., Harin, J. and Culotti, J. **Semaphorin and Eph receptor signaling guide a series of cell movements for ventral enclosure in C. elegans.** Curr. Biol. 2012, 22: 1-11.

Kamath, R. S., Fraser, A. G., Dong, Y., Poulin, G., Durbin, R., Gotta, M., Kanapin, A., Le Bot, N., Moreno, S., Sohrmann, M., Welchman, D. P., Zipperlen, P. and Ahringer, J. **Systematic functional analysis of the Caenorhabditis elegans genome using RNAi.** Nature. 2003, 421: 231-237.

Kawano, Y., Fukata, Y., Oshiro, N., Amano, M., Nakamura, T., Ito, M., Matsumura, F., Inagaki, M. and Kaibuchi, K. **Phosphorylation of myosin-binding subunit (MBS) of myosin phosphatase by Rho-kinase in vivo.** J. Cell Biol. 1999, 147: 1023-1038.

Kimura, K., Ito, M., Amano, M., Chihara, K., Fukata, Y., Nakafuku, M., Yamamori, B., Feng, J., Nakano, T., Okawa, K., Iwamatsu, A. and Kaibuchi, K. **Regulation of myosin phosphatase by Rho and Rho-associated kinase (Rho-kinase).** Science. 1996, 273: 245-248.

Kobielak, A. and Fuchs, E. **Alpha-catenin: at the junction of intracellular adhesion and actin dynamics.** Rev. Mol. Cell Biol. 2004, 5: 614-625.

Koppen, M., Simske, J. S., Sims, P. A., Firestein, B. L., Hall, D. H., Radice, A. D., Rongo, C. and Hardin, J. D. **Cooperative regulation of AJM-1 controls junctional integrity in Caenorhabditis elegans epithelia.** Nat. Cell Biol. 2001, 3: 983-991.

Kovar, D. R. **Molecular details of formin-mediated actin assembly.** Curr. Opin. Cell Biol. 2006, 18: 11-17.

Kurisu, S. and Takenawa, T. **The WASP and WAVE family proteins.** Genome Biol. 2009, 10: 226.

Labouesse, M. **Epithelial junctions and attachments**. *WormBook.* 2006, online review: 1-16.

Li, F. and Higgs, H. N. **Dissecting requirements for auto-inhibition of actin nucleation by the formin, mDia1.** J. Biol. Chem. 2005, 280: 6986-6992.

Lin, L., Tran, T., Hu, S., Cramer, T., Komuniecki, R. and Steven, R. M. **RHGF-2 is an essential Rho-1 specific RhoGEF that binds to the multi-PDZ domain scaffold protein MPZ-1 in Caenorhabditis elegans.** PLoS One. 2012, 7: e31499.

Machesky, L. M. and Insall, R. H. **Scar1 and the related Wiskott–Aldrich syndrome protein, WASP, regulate the actin cytoskeleton through the Arp2/3 complex.** Curr. Biol. 1998, 8: 1347-56.

Mackay, D. J., Nobes, C. D. and Hall, A. **The Rho's progress: a potential role during neuritogenesis for the Rho family of GTPases.** Trends Neurosci. 1995, 18: 496-501.

Maddox, A. S., Habermann, B., Desai, A. and Oegema, K. **Distinct roles for two C. elegans anillins in the gonad and early embryo.** Development. 2005, 132: 2837-2848.

Maddox, A. S., Lewellyn, L., Desai, A. and Oegema, K. **Anillin and the septins promote asymmetric ingression of the cytokinetic furrow.** Dev. Cell. 2007, 12: 827-835.

Mains, P. E., Kemphues, K. J., Sprunger, S. A., Sulston, I. A. and Wood, W. B. **Mutations affecting the meiotic and mitotic divisions of the early Caenorhabditis elegans embryo.** Genetics. 1990, 126: 593-605.

Matsumura, F. **Regulation of myosin II during cytokinesis in higher eukaryotes.** Trends Cell Biol. 2005, 15: 371-377.

Mullins, R. D., Heuser, J. A. and Pollard T. D. **The interaction of Arp2y3 complex with actin: Nucleation, high affinity pointed end capping, and formation of branching networks of filaments.** Proc Natl Aca Sci. 1998, 95: 6181-6186.

Nance, J., Lee J. Y. and Goldstein, B. **Gastrulation in C.elegans.** WormBook. 2005, online review: 1-13.

Oegema, K., Savoian, M. S., Mitchison, T. J. and Field, C. M. **Functional analysis of a human homologue of the Drosophila actin binding protein anillin suggests a role in cytokinesis.** J. Cell Biol. 2000, 150: 539-552.

Patel, F. B., Bernadskaya, Y. Y., Chen, E., Jobanputra, A., Pooladi, Z., Freeman, K. L., Gally, C., Mohler, W.A. and Soto, M. C. **The WAVE/SCAR complex promotes polarized cell movements and actin enrichment in epithelia during C. elegans embryogenesis.** Dev. Biol. 2008, 324: 297-309.

Paul, A. D. and Pollard, T. D. **Review of the mechanism of processive actin filament elongation by formins.** Cell Motil. Cytoskeleton. 2009, 66: 606-617.

Pestonjamasop, K. N., Forster, C., Sun, C., Gardiner, E. M., Bohl, B., Weiner, O., Bokock, G. M. and Glogauer, M. **Rac1 links leading edge and uropod events through Rho and myosin activation during chemotaxis.** Blood. 2006, 108: 2814-2820.

Pettitt, J., Cox, E. A., Broadbent, I. D., Flett, A. and Hardin, J. **The Caenorhabditis elegans p120 catenin homologue, JAC-1, modulates cadherin-catenin function during epidermal morphogenesis.** J. Cell Biol. 2003, 162: 15-22.

Piekny, A. J., Wissmann, A. and Mains, P. E. **Embryonic morphogenesis in Caenorhabditis elegans integrates the activity of LET-502 Rho-binding kinase, MEL-11 myosin phosphatase, DAF-2 insulin receptor and FEM-2 PP2c phosphatase.** Genetics. 2000, 156: 1671-1689.

Piekny, A. J. and Mains, P. E. **Rho-binding kinase (LET-502) and myosin phosphatase (MEL-11) regulate cytokinesis in the early Caenorhabditis elegans embryo.** J. Cell Sci. 2002, 115: 2271-2282.

Piekny, A. J., Johnson, J. L., Cham, G. D. and Mains, P. E. **The Caenorhabditis elegans nonmuscle myosin genes nmy-1 and nmy-2 function as redundant components of the**

let-502/Rho-binding kinase and mel-11/myosin phosphatase pathway during embryonic morphogenesis. Development. 2003, 130: 5695-5704.

Piekny, A. J. and Mains, P. E. **Squeezing an egg into a worm: C. elegans embryonic morphogenesis.** SWJ. 2003, 3: 1370-1381.

Piekny, A. J., Werner, M. and Glotzer, M. **Cytokinesis: welcome to the Rho zone.** Trends Cell Biol. 2005, 15: 651-658.

Piekny, A. J. and Glotzer, M. **Anillin is a scaffold protein that links RhoA, actin and myosin during cytokinesis.** Curr. Biol. 2008, 18: 30-36.

Piekny, A. J. and Maddox, A. S. **The myriad roles of Anillin during cytokinesis.** Sem. Cell Dev. Biol. 2010, 21: 881-891.

Pollard, T. D., Blanchoi, L. and Mullins, R. D. **Molecular mechanisms controlling actin filaments dynamics in nonmuscle cells.** Annu. Rev. Biophys. Biomol. Struct. 2000, 29: 545-576.

Pollard, T. D. and Cooper, J. A. **Actin, a central player in cell shape and movement.** Science. 2009, 326: 1208-1212.

Priess, J. R. and Hirsh, D. I. **Caenorhabditis elegans morphogenesis: the role of the**

cytoskeleton in elongation of the embryo. Dev. Biol. 1986, 117: 156-173.

Quinn, C. C., Pfeil, D. S. and Wadsworth, W. G. **CED-10/Rac1 mediates axon guidance by regulating the asymmetric distribution of MIG-10/lamellipodin.** Curr. Biol. 2008, 18: 808-813.

Raich, W. B., Agbunag, C. and Hardin, J. **Rapid epithelial-sheet sealing in the Caenorhabditis elegans embryo requires cadherin-dependent filopodial priming.** Curr. Biol. 1999, 9: 1139-1146.

Ridley, A. J., Paterson, H. F., Johnston, C. L., Diekmann, D. and Hall, A. **The small GTP-binding protein rac regulates growth factor-induced membrane ruffling.** Cell. 1992, 70: 401-410.

Roh-Johnson, M., Shemer, G., Higgins, C. D., McClellan, J. H., Werts, A. D., Tulu, U. S., Gao, L., Betzig, E., Kiehart, D. P. and Goldstein, B. **Triggering a cell shape change by exploiting preexisting actomyosin contractions.** Science. 2012, 335: 1232-1235.

Rossman, K. L., Der, C. J. and Sondek, J. **GEF means go: turning on RHO GTPases with guanine nucleotide-exchange factors.** Nat. Rev. Mol. Cell Biol. 2005, 6: 167-180.

Sawa, M., Suetsguru, S., Sugimoto, A., Miki, H., Yamamoto, M. and Takenawa, T. **Essential role of the C. elegans Arp2/3 complex in cell migration during ventral**

enclosure. J. Cell Sci. 2003, 116: 1505-1518.

Simske, J. S. and Hardin, J. **Getting into shape: epidermal morphogenesis in Caenorhabditis elegans embryos.** Bioessays. 2001, 23: 12-23.

Somers, W. G. and Saint, R. **A RhoGEF and Rho family GTPase-activating protein complex links the contractile ring to cortical microtubules at the onset of cytokinesis.** Dev. Cell. 2003, 4: 29-39.

Somlyo, A. P. and Somlyo, A. V. **Signal transduction by G-proteins, rho-kinase and protein phosphatase to smooth muscle and non-muscle myosin II.** J. Phys. 2000, 522: 177-185.

Soto, M. C., Qadota, H., Kasuya, K., Inoue, M., Tsuboi, D., Mello, C. C. and Kaibuchi, K. **The GEX-2 and GEX-3 proteins are required for tissue morphogenesis and cell migrations in C. elegans.** Genes Dev. 2002, 16: 620-632.

Straight, A. F., Field, C. M. and Michitson, T. J. **Anillin binds Nonmuscle myosin II and regulates the contractile ring.** Mol. Biol. Cell. 2005, 16: 193-201.

Sulston, J. E and Horvitz, H. R. **Post-embryonic cell lineages of the nematode, Caenorhabditis elegans.** Dev. Biol. 1977, 56: 110-156.

Sulston, J. E., Schierenberg, E., White, J. G. and Thomson, J. N. **The embryonic cell lineage of the nematode Caenorhabditis elegans.** Dev. Biol. 1983, 100: 64-119.

Swan, K. A., Severson, A. F., Carter, C. J., Martin, P. R., Schnabel, H., Schnabel, R. and Bowerman, B. **cyk-1: a C. elegans FH gene required for a late step in embryonic cytokinesis.** J. Cell Sci. 1998, 111: 2017-2027.

Symons, M., Derry, J. M., Karlak, B., Jiang, S., Lemahieu, V., Mccormick, F., Francke, U. and Abo, **A. Wiskott-Aldrich syndrome protein, a novel effector for the GTPase CDC42Hs, is implicated in actin polymerization.** Cell. 1996, 84: 723-734.

Tapon, N. and Hall, A. **Rho, Rac and Cdc42 GTPases regulate the organization of the actin cytoskeleton.** Curr. Opin. Cell Biol. 1997, 9: 86-92.

Torres, E., Rosen, M. K. **Protein-tyrosine Kinase and GTPase Signals Cooperate to Phosphorylate and Activate Wiskott-Aldrich Syndrome Protein (WASP)/Neuronal WASP.** J. Biol Chem. 2006, 281: 3513-3520.

Totsukawa, G., Yamakita, Y., Yamashiro, S., Hartshorne, D. J., Sasaki, Y. and Matsumuta, F. **Distinct roles of ROCK (Rho-kinase) and MLCK in spatial regulation of MLC phosphorylation for assembly of stress fibers and focal adhesions in 3T3 fibroblasts.** J. Cell Biol. 2000, 150: 797-806.

Tse, Y. C., Piekny, A. J. and Glotzer, M. **Anillin promotes astral microtubule-directed cortical myosin polarization.** Mol. Biol. Cell. 2011, 22: 3165-3175.

Vicente-Manzanares, M., Ma, X., Adelstein, R. S. and Horwitz A. R. **Non-muscle myosin II takes centre stage in cell adhesion and migration.** Nat. Rev. Mol. Cell Biol. 2009, 10: 778-790.

Wang, X., Roy, P. J., Holland, S. J., Zhang, L. W., Culotti, J. G. and Pawson, T. **Multiple Ephrins Control Cell Organization in C. elegans Using Kinase-Dependent and -Independent Functions of the VAB-1 Eph Receptor.** Mol. Cell. 1999, 4: 903-913.

Welch, M. D., DePace, A. H., Verma, S., Iwamatsu, A. and Mitchison, T. J. **The human Arp2/3 complex is composed of evolutionarily conserved subunits and is localized to cellular regions of dynamic actin filament assembly.** J. Cell Biol. 1997, 138: 375-384.

Williams-Masson, E. M., Malik, A. N. and Hardin, J. **An actin-mediated two-step mechanism is required for ventral enclosure of the C. elegans hypodermis.** Development. 1997, 124: 2889-2901.

Williams-Masson, E. M., Heid, P. J., Lavin, C. A. and Hardin, J. **The cellular mechanism of epithelial rearrangement during morphogenesis of the Caenorhabditis elegans dorsal hypodermis.** Dev. Biol. 1998, 204: 263-276.

Wissmann, A., Ingles, J., McGhee, J. D. and Mains, P. E. **Caenorhabditis elegans LET-502 is related to Rho-binding kinases and human myotonic dystrophy kinase and interacts genetically with a homolog of the regulatory subunit of smooth muscle myosin phosphatase to affect cell shape.** Genes Dev. 1997, 11: 409-422.

Wissmann, A., Ingles, J. and Mains, P. E. **The Caenorhabditis elegans mel-11 myosin phosphatase regulatory subunit affects tissue contraction in the somatic gonad and the embryonic epidermis and genetically interacts with the Rac signaling pathway.** Dev. Biol. 1999, 209: 111-127.

Withee, J., Galligan, B., Hawkins, N. and Garriga, G. **Caenorhabditis elegans WASP and Ena/VASP proteins play compensatory roles in morphogenesis and neuronal cell migration.** Genetics. 2004, 167: 1165-1176.

Yamashiro, S., Totsukawa, G., Yamakita, Y., Sasaki, Y., Madaule, P., Ishizaki, T., Narumiya, S. and Matsumura, F. **Citron kinase, a Rho-dependent kinase, induces di-phosphorylation of regulatory light chain of myosin II.** Mol. Biol. Cell. 2003, 14: 1745-1756.

Yasui, Y., Amano, M., Nagata, K., Inagaki, N., Nakamura, H., Sava, H., Kaibuchi, K. and Inagaki, M. **Roles of Rho-associated Kinase in Cytokinesis; Mutations in Rho-**

associated Kinase Phosphorylation Sites Impair Cytokinetic Segregation of Glial Filaments. *JCB. 1998,* 143: 1249-1258

Yuce, O., Piekny, A. and Glotzer, M. **An ECT2-centralspindlin complex regulates localization and function of RhoA.** J. Cell Biol. 2005, 170: 571-582.

Zhang, H., Gally, C., Labouesse, M. **Tissue morphogenesis: how multiple cells cooperate to generate a tissue.** Curr. Opin. Cell Biol. 2010, 22: 575-582.

Zhang, L. and Maddox, A. S. **Anillin. Curr**. Biol. 2010, 20: 135-136.

aZhao, W. M. and Fang, G. **Anillin is a substrate of anaphase-promoting complex/cyclosome (APC/C) that controls spatial contractility of myosin during late cytokinesis.** J. Biol. Chem. 2005, 280: 33516-33524.

bZhao, W. M and Fang, G. **MgcRacGap controls the assembly of the contractile ring and the initiation of cytokinesis.** Proc. Natl. Sci. USA. 2005, 102: 13158-13163.